Electronic Supplementary Information

Reversible photochromic switching in a Ru(II) polypyridyl complex

Duenpen Unjaroen, Johan B. Kasper and Wesley R. Browne*

Contents

Experimental section

Instrumentation

Raman spectra were recorded and irradiations carried out at 457 nm (Cobolt Lasers 50 mW), 405 nm (Ondax 50 mW) and 355 nm (Cobolt Lasers 7 mW), in 1 cm pathlength quartz cuvettes. The excitation beam was focused at the sample using a 10 cm focal length parabolic mirror at ca. 35° with respect to the collection axis. The Raman scattering was collected and collimated with a 2.5 cm diameter, 15 mm focal length plano convex mirror, filtered to remove Rayleigh scattering using an appropriate Steep Edge long pass filter (Semrock), and focused into the spectrograph (Shamrock 303, AndorTechnology, 1800 1200 l/mm grating blazed at 500 nm), and imaged onto a Andor iDus-420-BEX2-DD CCD camera. Raman spectra at 785 nm were recorded using a Perkin Elmer Raman station. FTIR spectra were recorded on a Perkin Elmer Spectrum 2 equipped with a UATR attachment. UV/Vis absorption spectra were recorded on either a Specord S300 UV/Vis or S600 UV/Vis diode array spectrometer (AnalytikJena). Irradiation was monitored in situ using the same excitation sources as for Raman spectroscopy (*vide supra*) defocused to a 0.8 cm diameter beam incident at 90° to the monitoring beam. ^{1}H NMR (400.0MHz) spectra were recorded on a Varian Avance 400 NMR spectrometer. Chemical shifts are relative to CD_3CN (1.94 ppm). ESI-MS spectra were recorded on a Triple Quadrupole LC/MS/MS mass spectrometer (API 3000, Perkin-Elmer Sciex Instruments). Elemental analyses were performed with a Foss-Heraeus CHN Rapid or a EuroVector Euro EA elemental analyzer.

Synthesis

Complex **4**, [Ru(Cl)(MeN_4Py)]Cl, was prepared from 1,1-di(pyridin-2-yl)-N,N-bis(pyridin-2-ylmethyl)ethan-1-amine (**MeN_4Py**) and ruthenium chloride hydrate ($RuCl_3$. xH_2O). $RuCl_3$ xH_2O (122.4 mg, 0.59 mmol), **MeN_4Py** (100.1 mg, 0.26 mmol) and L-ascorbic acid (92.4 mg, 0.52 mmol) were heated at reflux overnight in EtOH/H_2O (2:3 v/v) and then cooled to room temperature. The solvent was removed *in vacuo* and the crude product purified by column chromatography on neutral alumina, eluting with CH_3CN to yield Ru(Cl)(MeN4Py)(Cl) **4** as a red solid (107.5 mg, 74%). ^{1}H NMR (400 MHz, CD_3CN) δ 9.35 (d, *J* = 5.4 Hz, 2H), 9.04 (d, *J* = 5.4 Hz, 2H), 7.88 (t, *J* = 7.7 Hz, 2H), 7.65 (d, *J* = 8.0 Hz, 2H), 7.54 (t, *J* = 7.7 Hz, 2H), 7.29 (t, *J* = 6.5 Hz, 2H), 7.24 (t, *J* = 6.6 Hz, 2H), 6.99 (d, *J* = 7.8 Hz, 2H), 4.19 (s, 4H), 2.23 (s, 3H). ESI/MS: m/z 518 $[M\text{-}Cl]^+$.

Complex **5**, [Ru(Cl)(MeN_4Py)](BF_4) was prepared by saturated aqueous $NaBF_4$ to a solution of **4** in water. **5** precipitated as a red solid. ^{1}H NMR (400 MHz, CD_3CN) δ 9.35 (d, *J* = 5.4 Hz, 2H), 9.04 (d, *J* = 5.4 Hz, 2H), 7.88 (t, *J* = 7.8 Hz, 2H), 7.64 (d, *J* = 8.0 Hz, 2H), 7.54 (t, *J* = 7.7 Hz, 2H), 7.29 (t, *J* = 6.4 Hz, 2H), 7.24 (t, *J* = 6.4 Hz, 2H), 6.98 (d, *J* = 8.0 Hz, 2H), 4.15 (q_{AB}, *J* = 18.6 Hz, 4H), 2.25 (s, 3H). ESI/MS: m/z 518 $[M\text{-}BF_4]^+$.

Water (1 mL) was added to the solution of **5** (65 mg, 0.11 mmol) in CH_3CN (9 mL) and the mixture heated at 55 ^{o}C. The reaction was cooled to room temperature after 6 h and the solvent reduced *in vacuo*. Addition of a few drop of saturated of $NaBF_4$ yielded **1** as a yellow solid (69.0 mg, 92%). ^{1}H NMR (400 MHz, CD_3CN) δ 8.94 (d, *J* = 5.4 Hz, 2H), 8.84 (d, *J* = 5.4 Hz, 2H), 7.97 (t, *J* = 7.7 Hz, 2H), 7.74 (d, *J* = 8.0 Hz, 2H), 7.64 (t, *J* = 7.8 Hz, 2H), 7.37 (t, *J* = 6.6 Hz, 2H), 7.29 (t, *J* = 6.6 Hz, 2H), 7.07 (d, *J* = 8.0 Hz, 2H), 4.36 (s, 4H), 2.73 (s, 3H), 2.32(s, 3H). ESI/MS: m/z 262 $[M\text{-}(BF_4)_2]^{2+}$. *Anal.* Calc. for $RuC_{26}H_{26}B_2F_8N_6$: C, 44.79; N, 12.06; H, 3.75. Found: C, 43.31; N, 11.75; H, 3.76%.

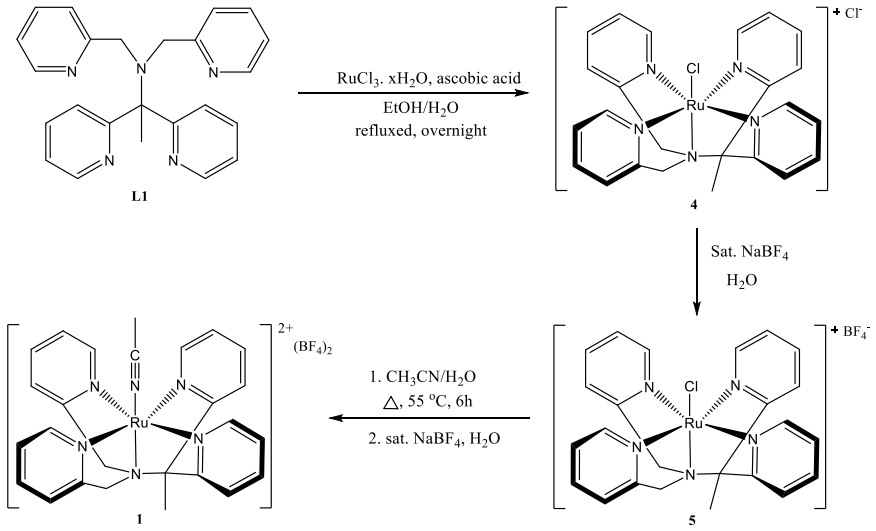

Scheme S1. Synthesis of $[Ru(CH_3CN)(MeN_4Py)](BF_4)_2$ (**1**).

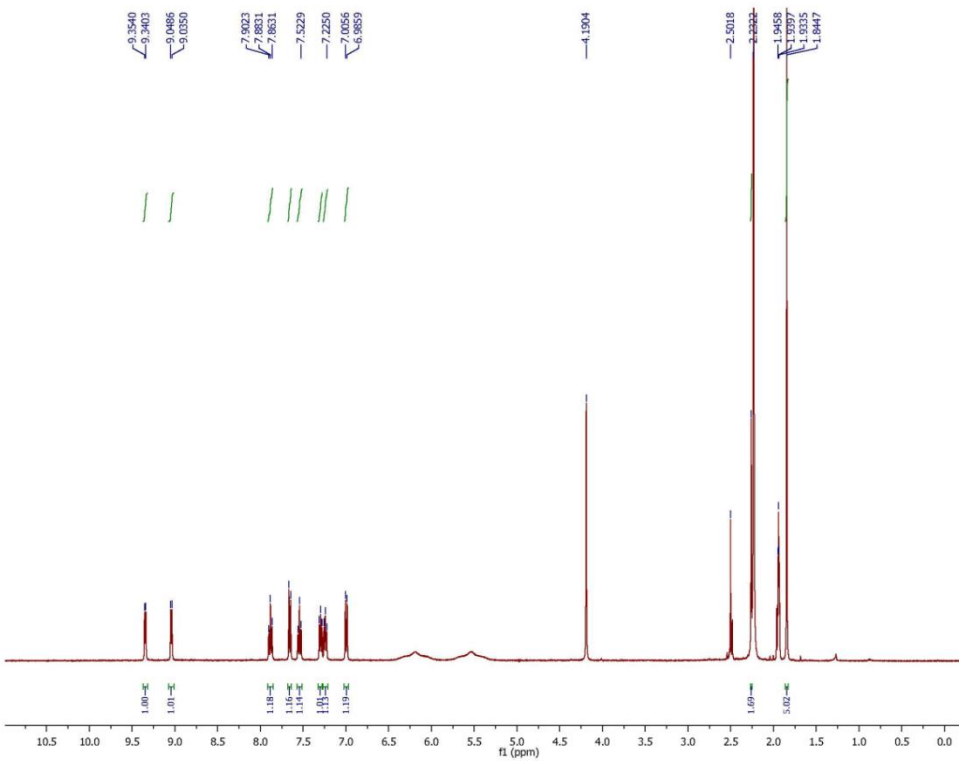

Fig. S1. ^{1}H NMR spectrum of complex **4** in CD_3CN.

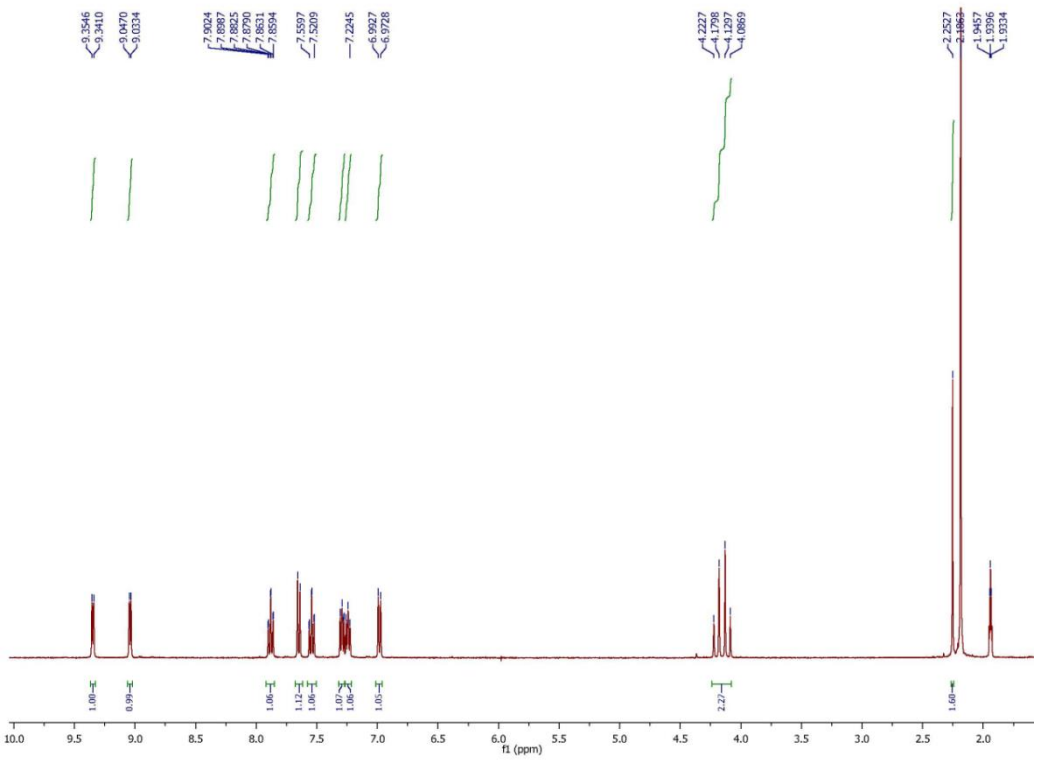

Fig. S2. ^{1}H NMR spectrum of complex **5** in CD_3CN.

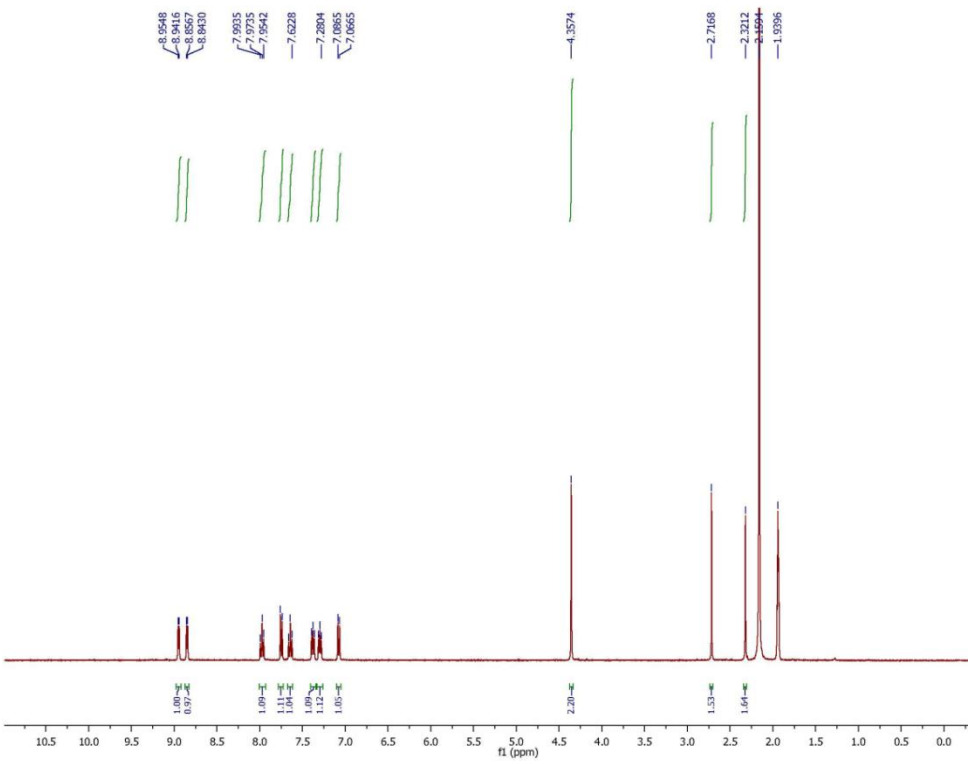

Fig. S3. ^{1}H NMR spectrum of complex **1** in CD_3CN.

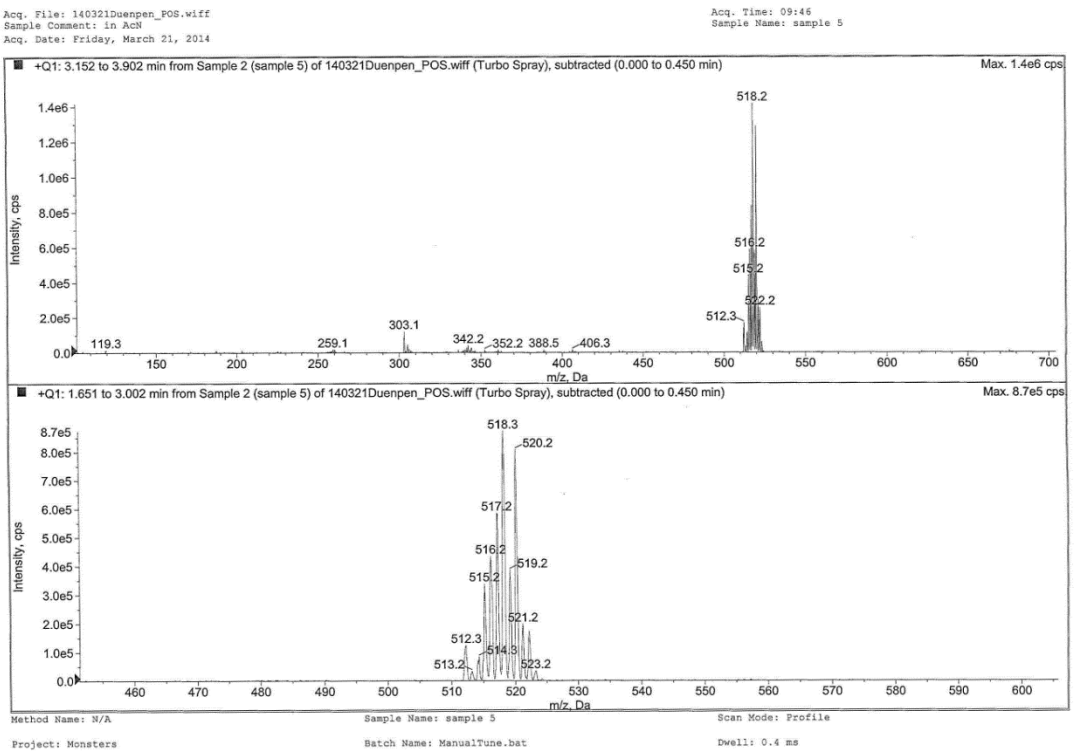

Fig. S4. ESI/MS spectrum of complex **4**.

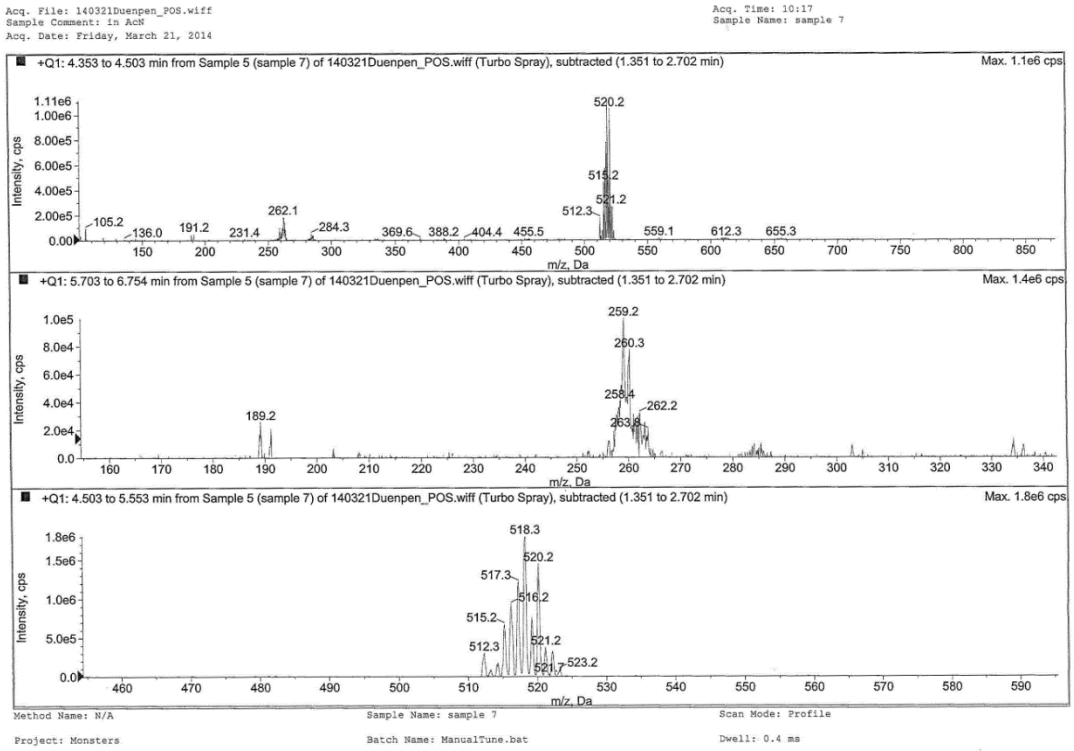

Fig. S5. ESI/MS spectrum of complex **5**.

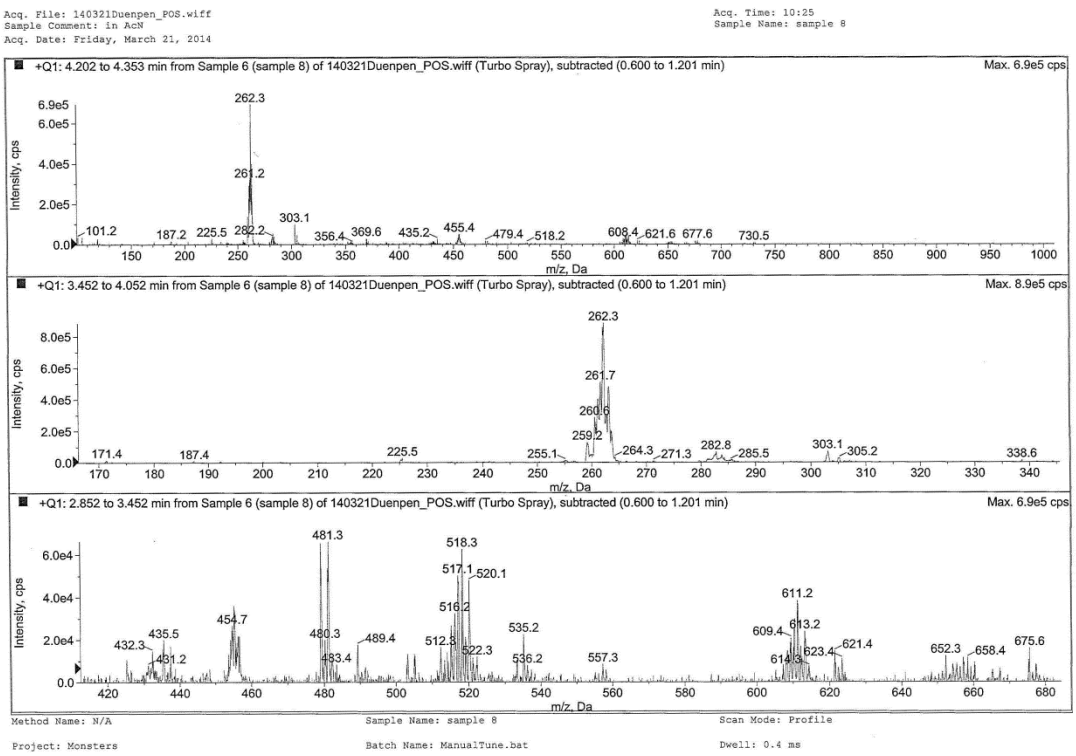

Fig. S6. ESI/MS spectrum of complex **1**.

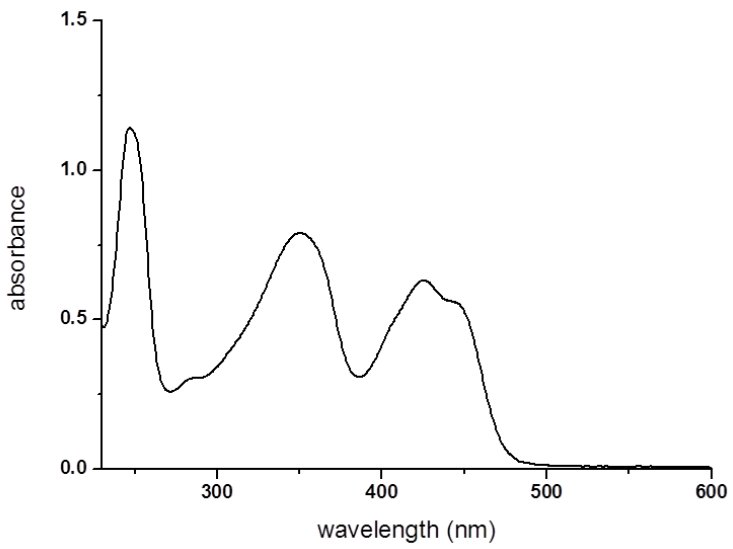

Fig. S7. UV/vis absorption spectrum of complex **1** in CH_3CN; λ 425 nm (ε = 8.13 × 10^3 M^{-1} cm^{-1}).

Raman and FTIR spectroscopy

The Raman spectrum at λ_{exc} 785 nm of **1** in the solid state reveals the vibrational band of CH_3CN at 2268 cm^{-1}. After evaporation of solvent of **3** in CD_3CN (generated by irradiation at 457 nm), the vibrational band of CH_3CN and CD_3CN at 2287 cm^{-1} and 2112 cm^{-1}, respectively, are observed. Similarly, the FTIR spectrum also shows the corresponding CH_3CN band at 2260 cm^{-1}. The bands in region 1600-1200 cm^{-1} are assigned to pyridine based vibrations by comparison with the Raman spectrum of $[Fe^{II}(MeN4Py)(CH_3CN)](ClO_4)_2$.[i]

Upon irradiation at 457 nm, the bands at 1285 and 1340 cm^{-1} decrease and a band at 1297 cm^{-1} appears, the latter of which is assigned to the pyridine group not coordinated to the Ru (II) ion.

The Raman spectrum of **1** in CD_3CN (0.1 mM) was monitored at the isosbestic point (λ_{exc} 405 nm). The band at 1297 cm^{-1} confirms the change in ligand denticity and after irradiation at 355 nm the spectrum corresponding to **1** in CD_3CN (without irradiation) is recovered (Fig. S12).

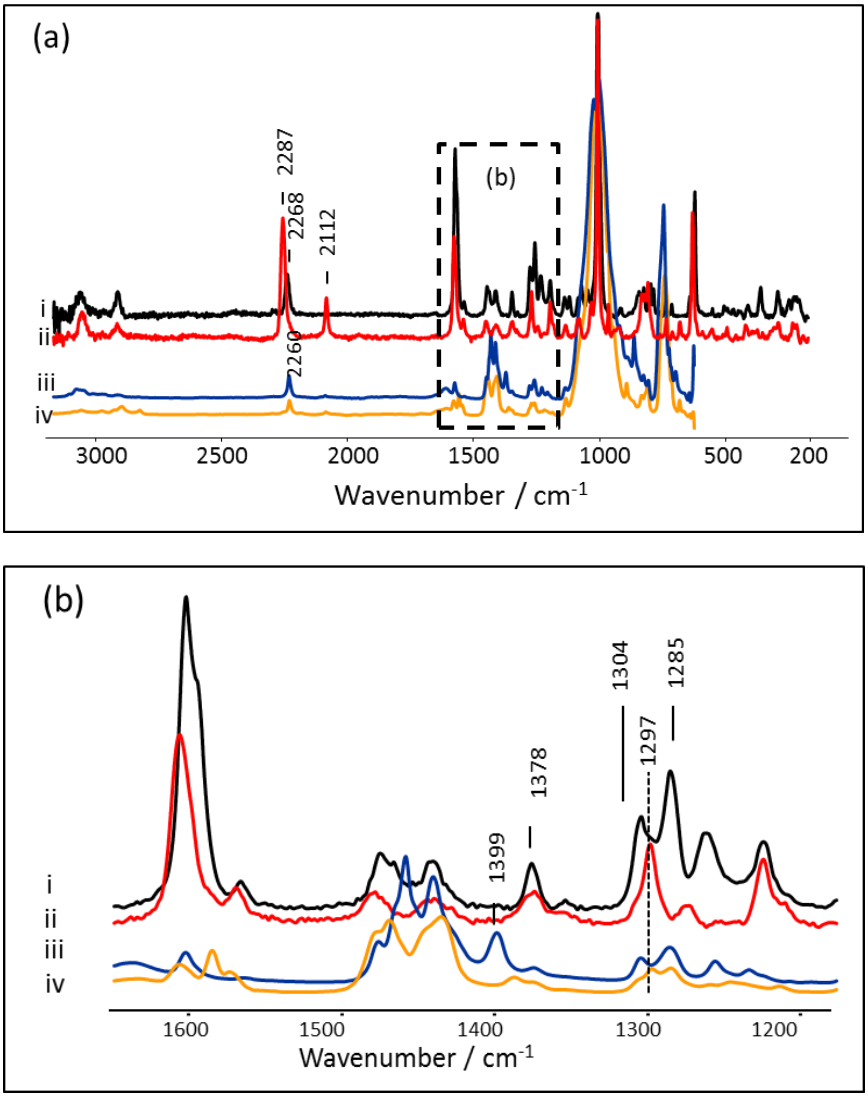

Fig. S8. (a) Raman spectrum (solid state) of **1** i) before irradiation at 457 nm ii) after irradiation at 457 mm iii) FTIR spectrum of **1** before irradiation at 457 nm iv) after irradiation at 457 nm. (b) Expansion of (a).

Photochemistry detected by ESI-MS

(**1**) $[Ru(CH_3CN)(MeN4Py)]^{2+}$ in CH_3CN (0.07 mM) was irradiation at λ 457 nm (18 min) to generate the corresponding complex (**2**) $[Ru(CH_3CN)_2(MeN4Py)]^{2+}$. The ESI-MS spectrum of **2** in CH_3CN shows signals at m/z 282. After subsequent irradiation at λ 355 nm (22 min) to form **1** and ESI-MS spectrum shows a peak at m/z 262 (Scheme S2).

Scheme S2. Photo-irradiation of (**1**) $Ru[(CH_3CN)(MeN4Py)]^{2+}$ in CH_3CN; irradiation at 457 nm and 355 nm.

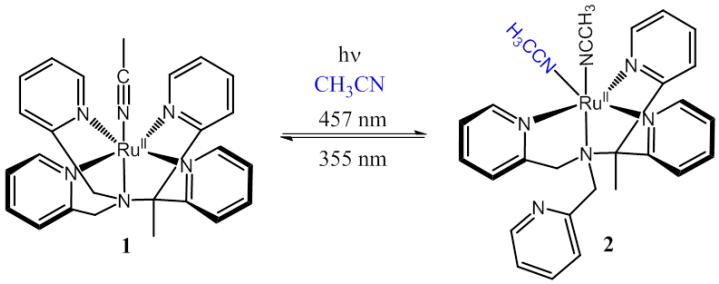

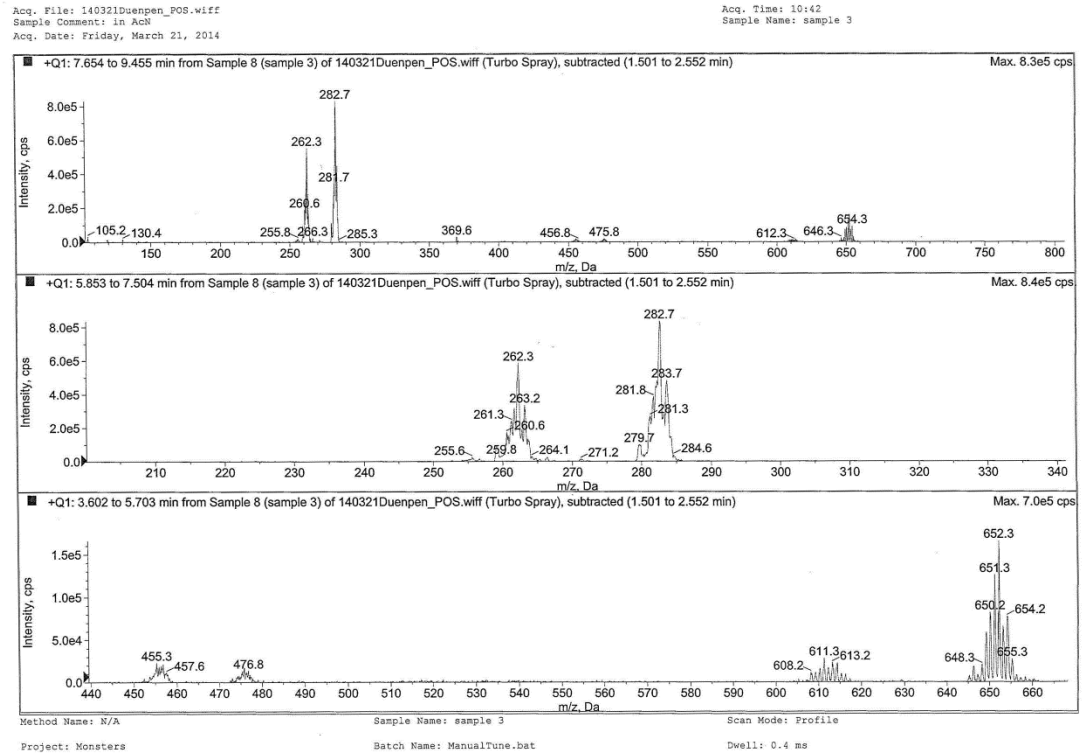

Fig. S9. ESI/MS spectrum of **1**in CH_3CN after irradiation at 457 nm, signals correspond to complex **2**.

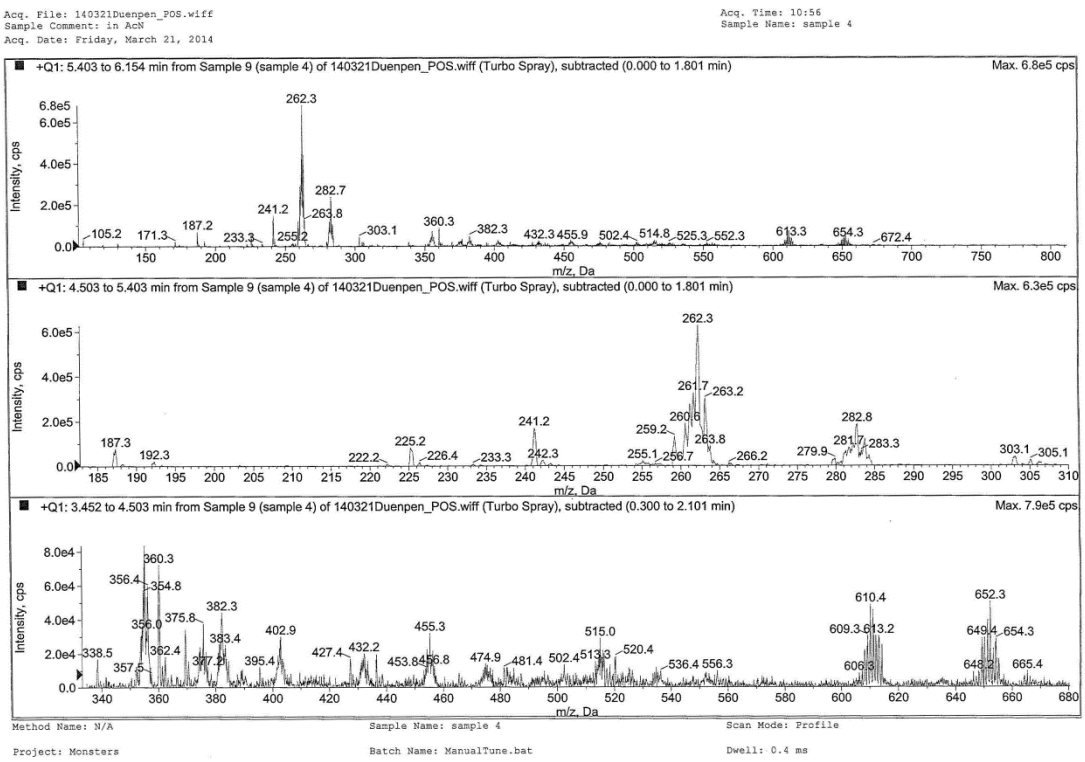

Fig. S10. ESI/MS spectrum of complex **2** in CH_3CN after irradiation at 355 nm, signals correspond to **1**.

Preparative photochemistry

1 ($[Ru(CH_3CN)(MeN4Py)]^{2+}$, 0.07 mM)) was irradiated in CD_3CN. Irradiation at 457 nm for 20 min gave a m/z 285 corresponding to $[Ru(CH_3CN)(CD_3CN)(MeN4Py)]^{2+}$. ^1H NMR (400 MHz, CD_3CN) δ 9.02 (d, *J* = 5.8 Hz, 1H), 8.83 (d, *J* = 5.6 Hz, 1H), 8.80 (d, *J* = 5.4 Hz, 1H), 8.75 (d, *J* = 4.4 Hz, 1H), 8.01 (t, *J* = 7.8 Hz, 1H), 7.88 (t, *J* = 7.8 Hz, 1H), 7.74, (t, *J* = 7.7 Hz, 1H), 7.64 (d, *J* = 8.0 Hz, 1H), 7.59 (m, 2H), 7.53 (d, *J* = 7.8 Hz, 1H), 7.44 (t, *J* = 6.8 Hz, 1H), 7.34 (t, *J* = 6.9 Hz, 1H), 7.26 (t, *J* = 6.6 Hz, 1H), 7.14 (d, *J* = 8.2 Hz, 1H), 6.79 (d, *J* = 7.6 Hz, 1H), 5.42 (d, *J* = 14.7 Hz, 1H), 5.21 (d, *J* = 15.0 Hz, 1H), 3.71 (d, *J* = 17.5 Hz, 1H), 3.31 (d, *J* = 17.7 Hz, 1H), 2.78 (s, 3H), 2.36 (s, 3H). Upon irradiation of **3** at 355 nm, the ESI/MS shows a peak at 262 corresponding to complex **1.**

Scheme S3. Photoirradiation of $[RuCH_3CN)(MeN4Py)]^{2+}$ in CD3CN;irradiation at 457 nm and 355 nm.

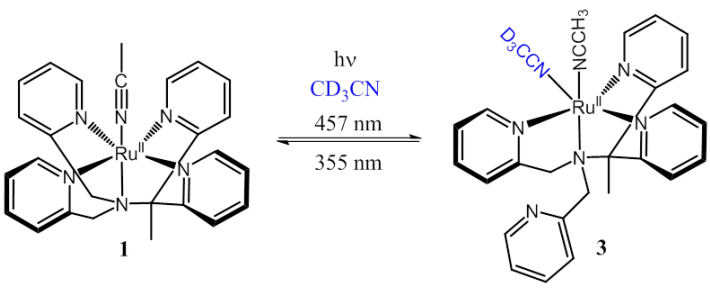

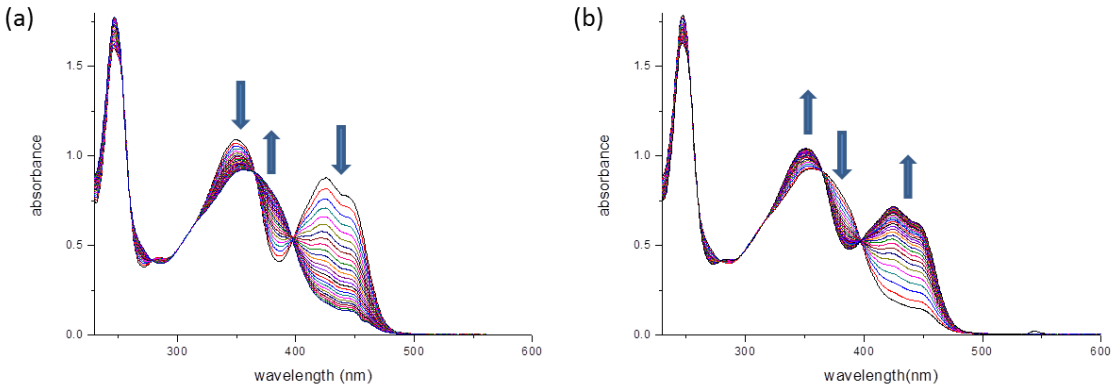

Fig. S11 Changes in UV/vis absorption spectrum of **1** in CD_3CN; irradiation at (a) 457 nm (b) 355 nm

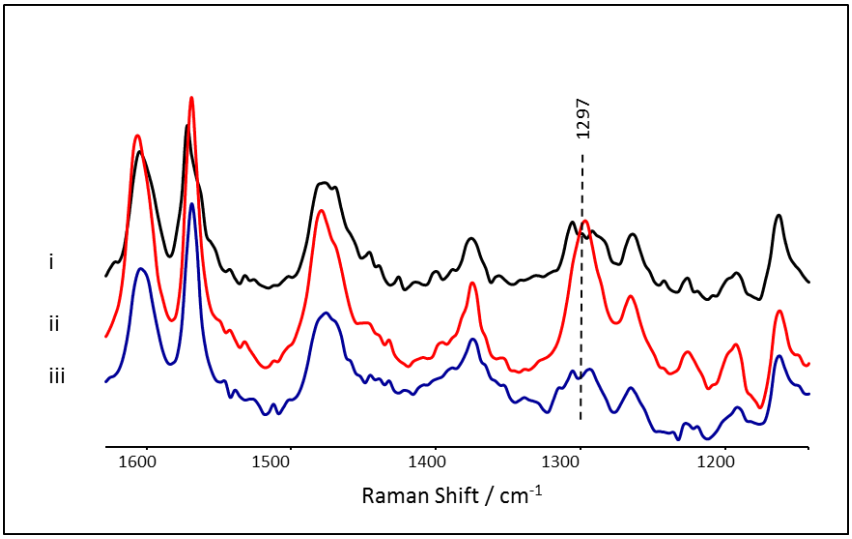

Fig. S12. Changes in Raman spectrum of **1** in CD_3CN i) before irradiation at 457 nm ii) after irradiation at 457 nm iii) after irradiation at 355 nm (λ_{exc} 405 nm).

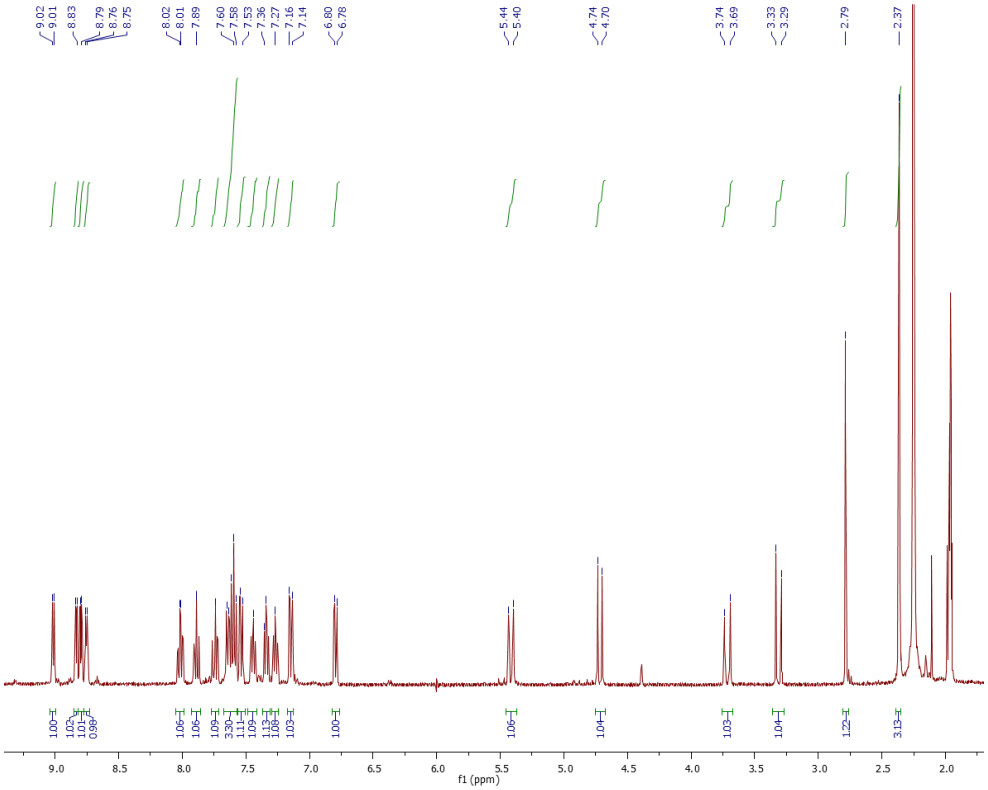

Fig. S13. ^{1}H-NMR spectrum of **1** in CD_3CN after irradiation at 457 nm corresponding to complex **3**.

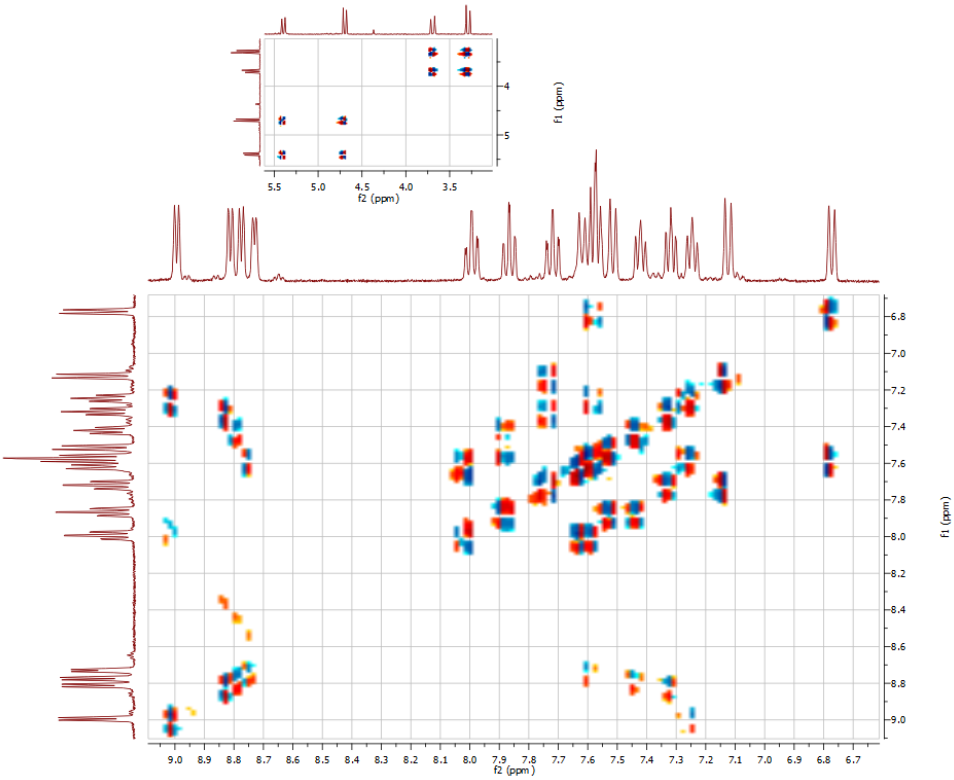

Fig. S14. DQF-COSY NMR spectrum of **1** in CD_3CN after irradiation at 457 nm corresponding to complex **3**.

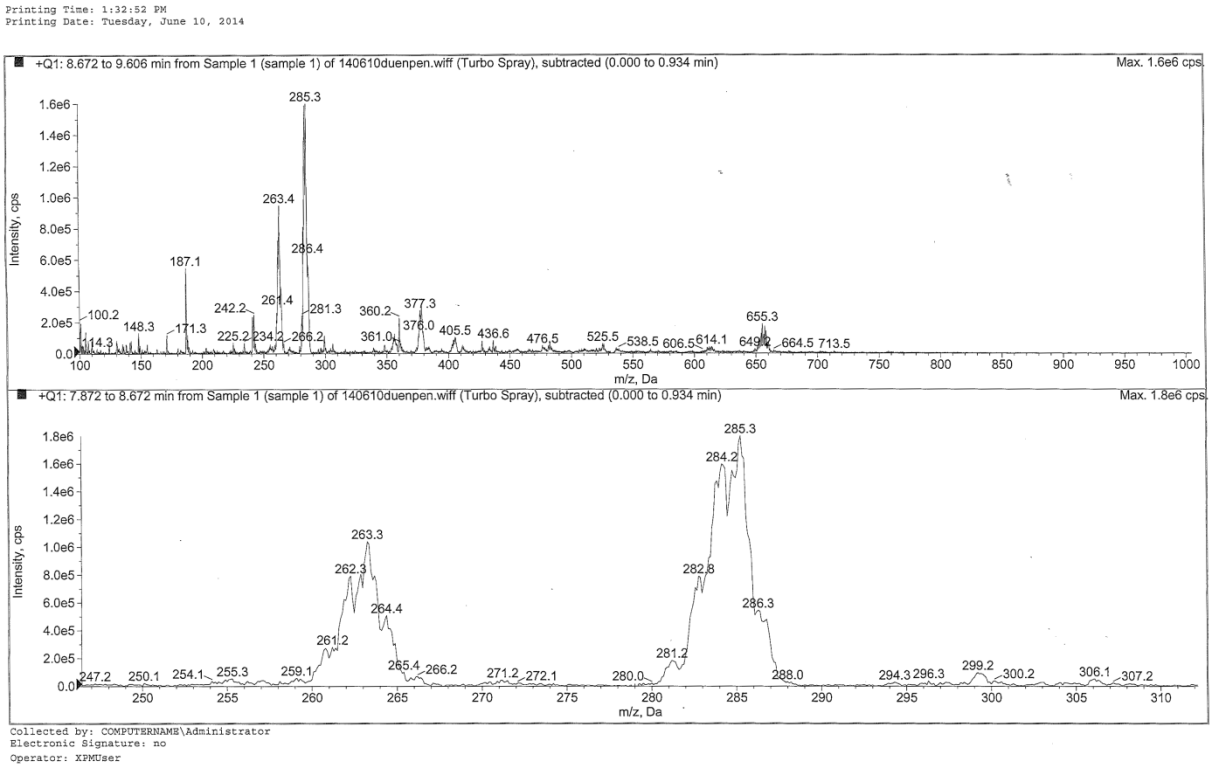

Fig. S15. ESI/MS spectrum of complex **1** in CD_3CN after irradiation at 457 nm corresponding to the complex **3**.

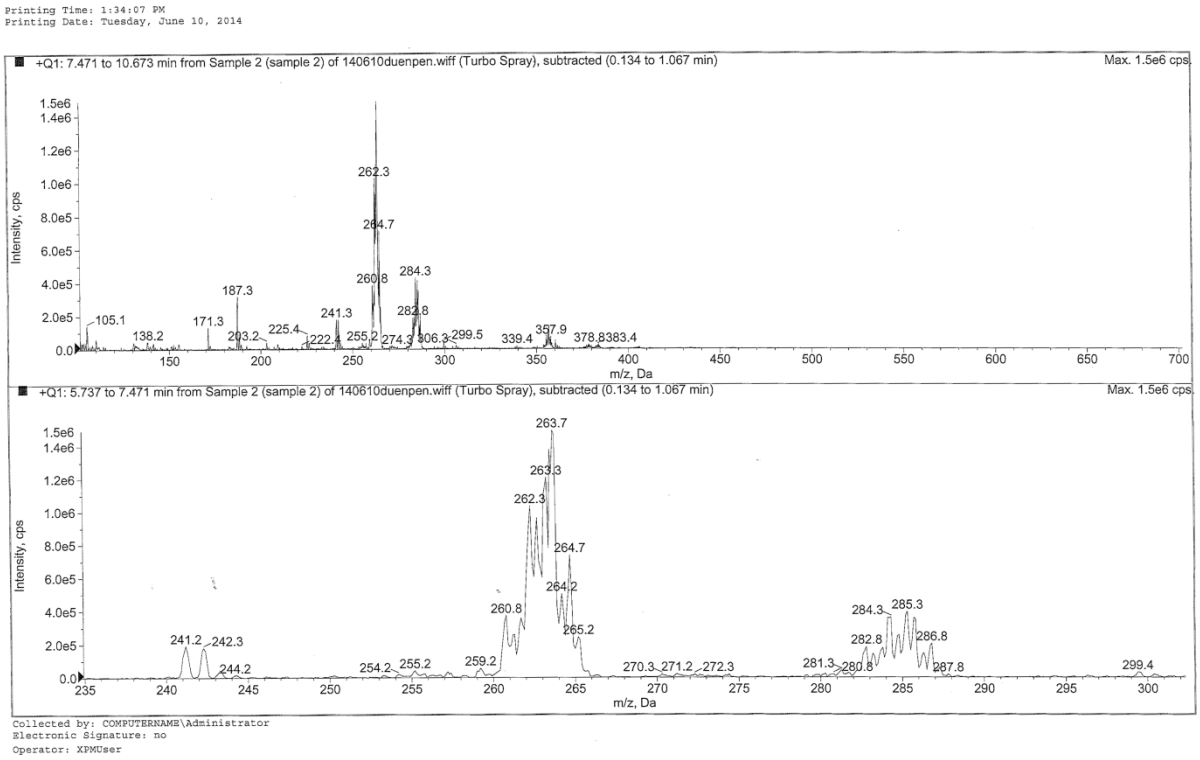

Fig. S16. ESI/MS spectrum of complex **3** in CD_3CN after irradiation at 355 nm corresponding to the complex **1**.

Photochemistry in other solvents

The effect of water and oxygen were examined in photoirradiation of $[Ru(CH_3CN)(MeN4Py)]^{2+}$ by addition of 1% H_2O in CH_3CN, anhydrous CH_3CN and Ar purged in CH_3CN (5 min) instead of CH_3CN as a solvent.

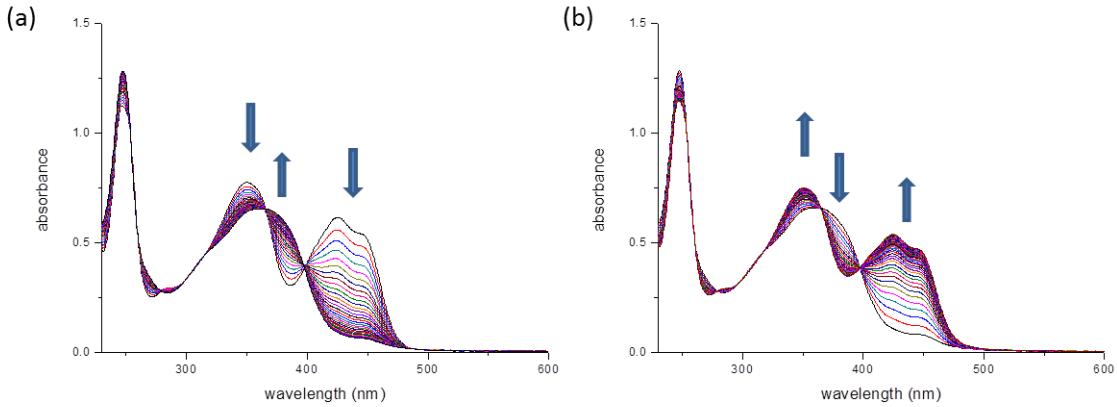

Fig. S17. Changes in UV/vis absorption spectrum of **1** in 1% H_2O in CH_3CN; irradiation at (a) λ 457 nm (b) λ 355 nm.

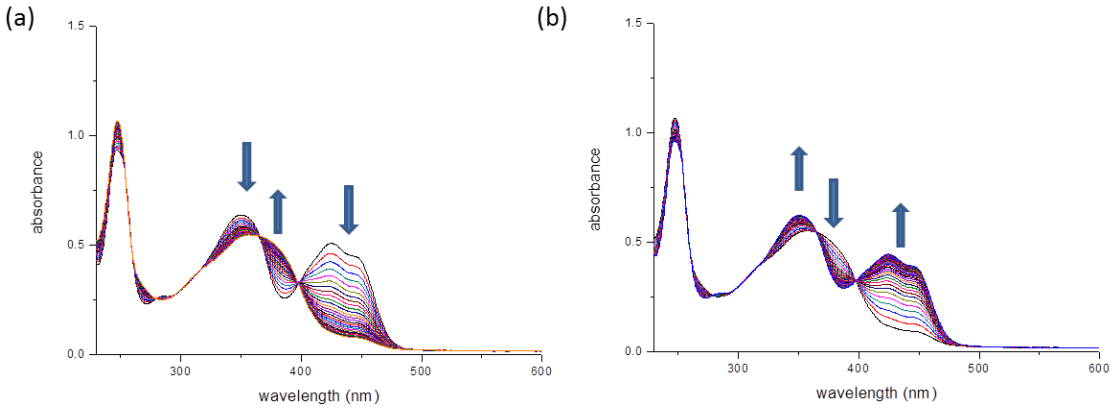

Fig. S18. Changes in UV/vis absorption spectrum of **1** in anhydrous CH_3CN; irradiation at (a) λ 457 nm (b) λ 355 nm.

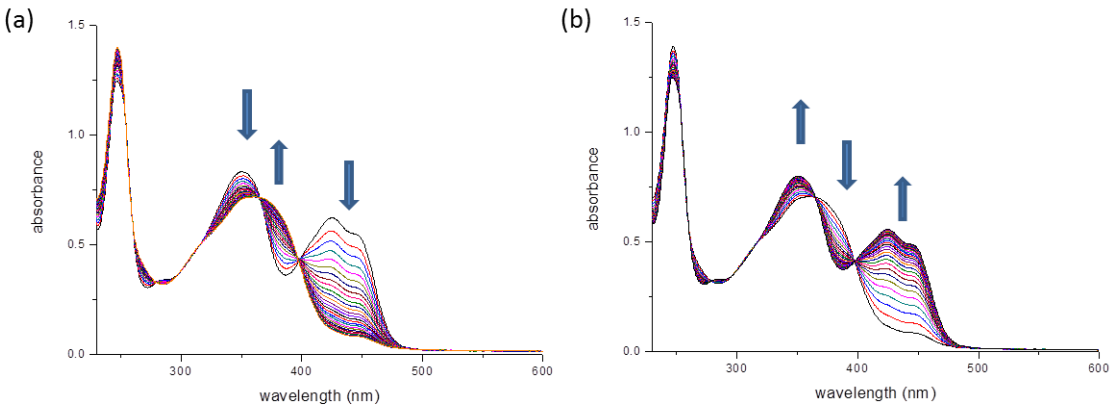

Fig. S19. Changes in UV/vis absorption spectrum of **1** in Ar purged CH_3CN (5 min); irradiation at (a) λ 457 nm (b) λ 355 nm.

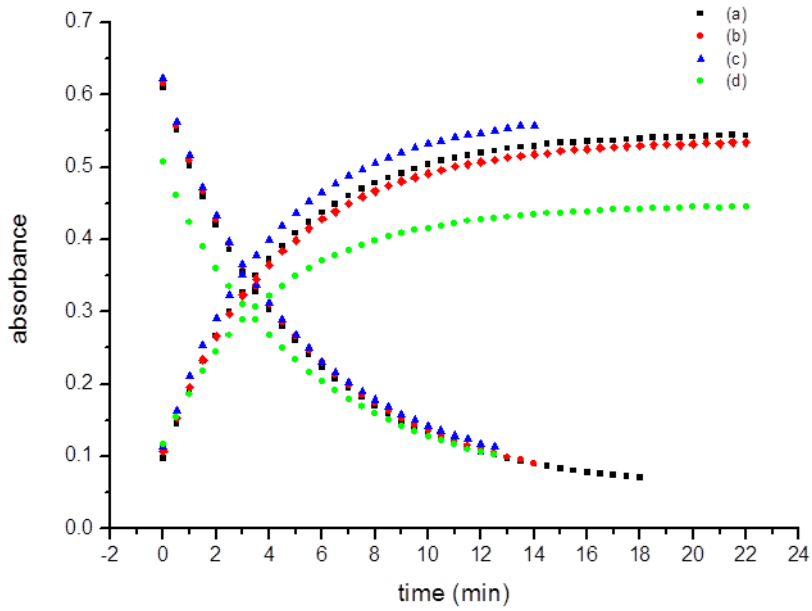

Fig. S20. Changes in absorbance at λ 425 nm of **1** when irradiation at 457 nm and 355 nm in (a) CH_3CN (b) 1% H_2O in CH_3CN (c) in Ar purged CH_3CN (d) anhydrous CH_3CN.

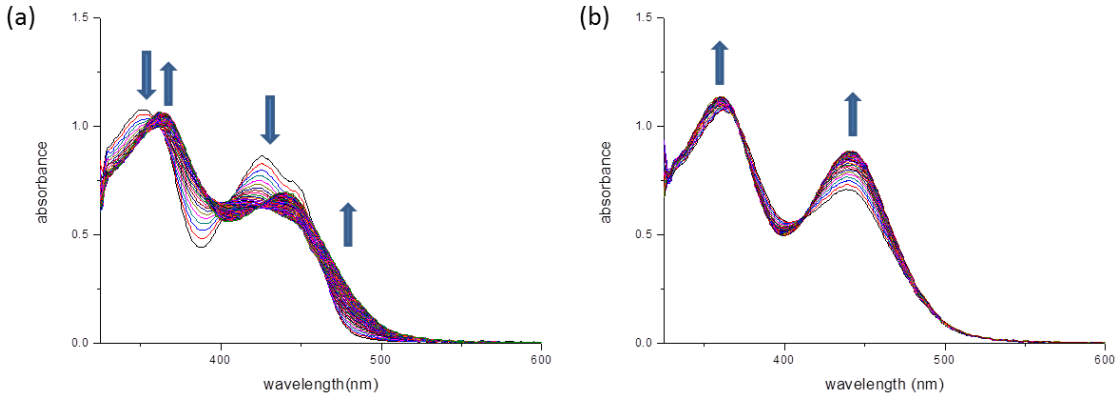

Fig. S21. Changes in UV/vis absorption spectrum of **1** in acetone; irradiation at (a) λ 457 nm (b) λ 355 nm

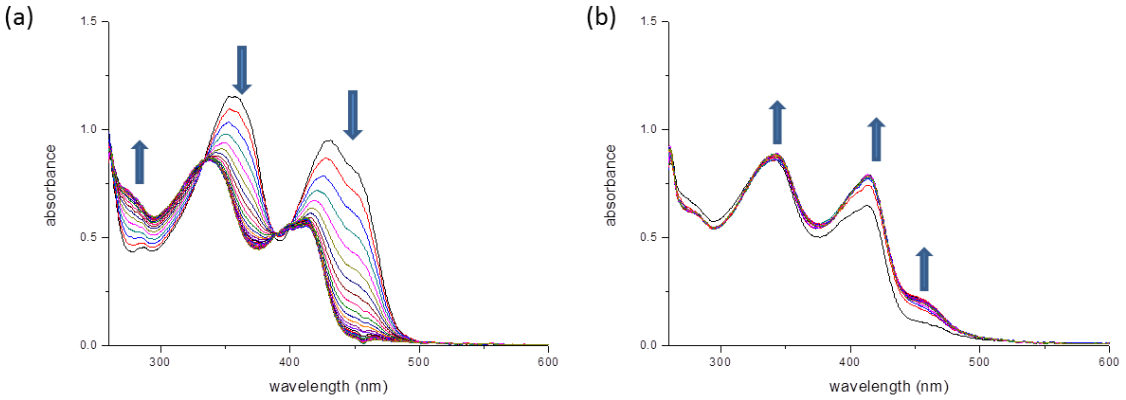

Fig S22. Changes in UV/vis absorption spectrum of **1** in DMSO; irradiation at (a) λ 457 nm (b) λ 355 nm.

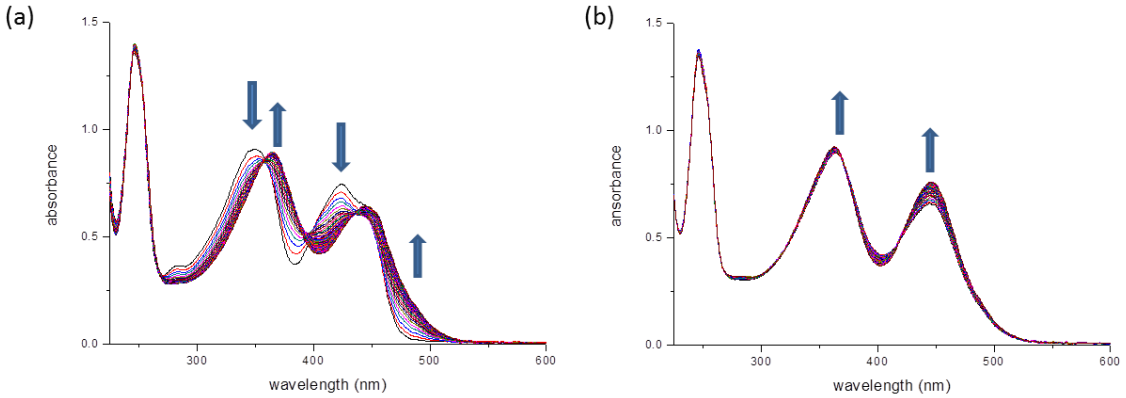

Fig. S23. Changes in UV/vis absorption spectrum of **1** in H_2O; irradiation at (a) λ 457 nm (b) λ 355 nm.

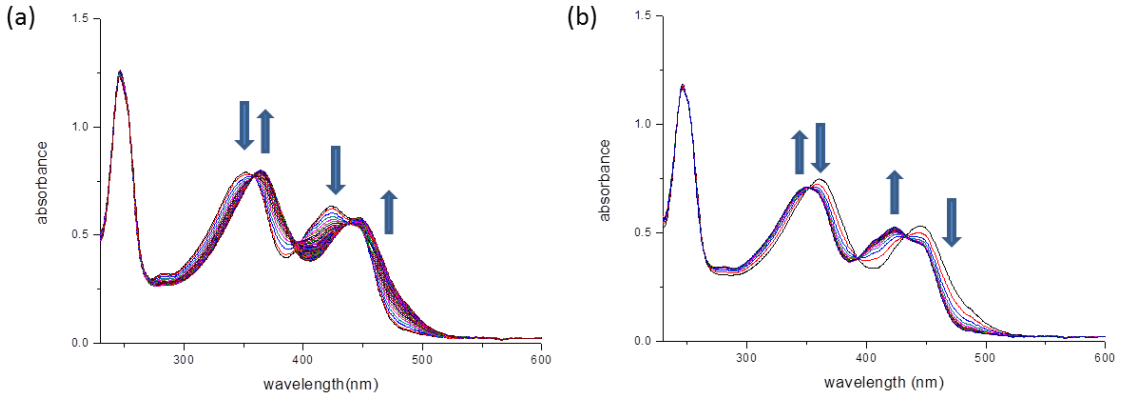

Figure 24. Changes in UV/vis absorption spectrum of **1** in H_2O; irradiation at (a) λ 457 nm (b) λ 355 nm after addition 5% CH_3CN.

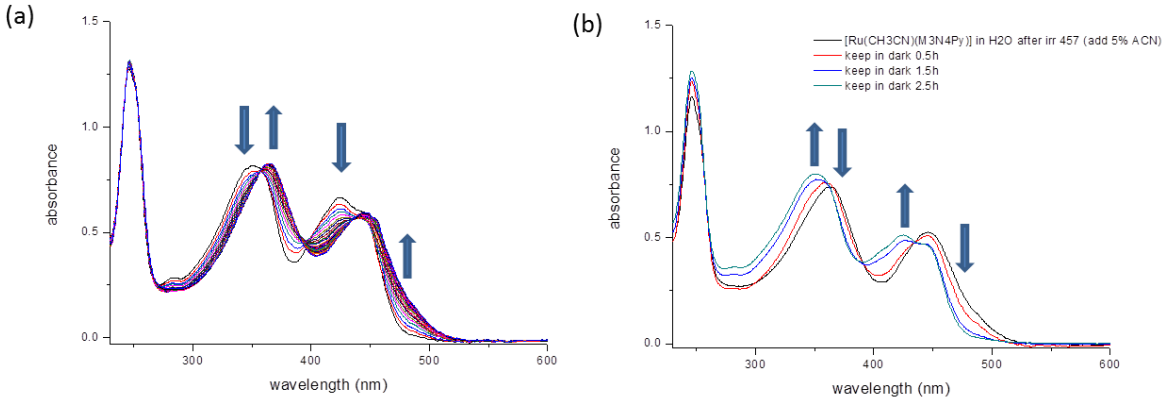

Fig. S25. Changes in UV/vis absorption spectrum of **1** in H_2O; irradiation at (a) λ 457 nm (b) addition 5% CH_3CN followed by holding in the dark.

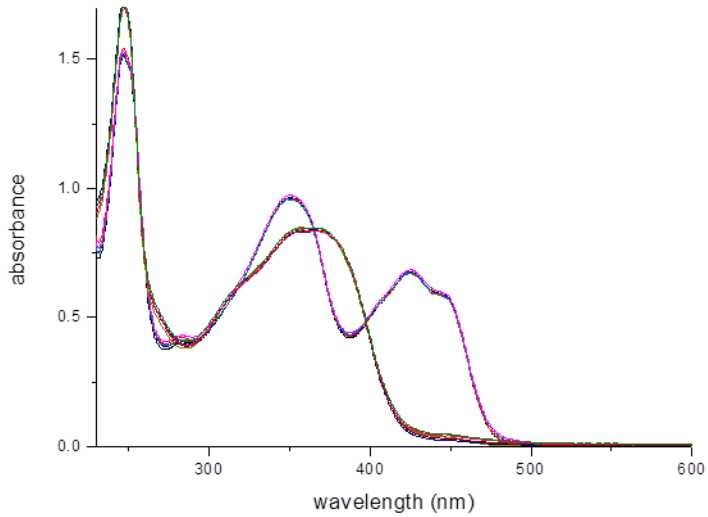

Fig. S26. UV/vis absorption spectrum of **1** in CH_3CN; after irradiation at λ 457 nm and then 355 nm (5 cycles) .

---

i A. Draksharapu, Q. Li, H. Logtenberg, T. A. van den Berg, A. Meetsma, J. S. Killeen, B. L. Feringa, R. Hage, G. Roelfes and W. R. Browne, *Inorg. Chem*. 2012, **51**, 900-9013.